Published by
NIGERIAN SOCIETY OF PHYSICAL SCIENCES
Available online @ https://journal.nsps.org.ng/index.php/jnsps

J. Nig. Soc. Phys. Sci. 9 (2027) 3527

Journal of the Nigerian Society of Physical Sciences

Statistical analysis of nuclear magnetic resonance relaxation parameters of rare deoxyribonucleic acid intermediates

John A. Lazarus[a,b,*], Michael O. Dada[a], Awojoyogbe O. Bamidele[a], Simon O. Abolarinwa[c]

[a]Department of Physics, Federal University of Technology, P.M.B. 65, Minna, Niger State, Nigeria
[b]Department of Physics, Ibrahim Badamasi Babangida University, P.M.B. 11, Lapai, Niger State, Nigeria
[c]Department of Animal Biology, Federal University of Technology, P.M.B. 65, Minna, Niger State, Nigeria

Abstract

Rare DNA intermediate structures are essential for biological processes in living organisms, including protein folding and unfolding, gene transcription, and replication. Studies have been conducted on DNA intermediate structures using different nuclear magnetic resonance (NMR) approaches, but NMR-based statistical analysis of DNA is less researched. Therefore, the current study presents a statistical analysis of NMR longitudinal (T_1) and transverse (T_2) relaxation times for rare DNA intermediate structures. Published experimental T_1 and T_2 datasets for five rare DNA intermediate structures were simulated using an R script to obtain 500 data points for each DNA structure; these were used to perform non-parametric statistical analysis using Wolfram Mathematica software. Results of the analysis show that the T_1 and T_2 datasets for each of the five rare DNA structures have distinct features. This highlights the possibility of utilising DNA T_1 and T_2 NMR parameters to isolate DNA structures responsible for regulating gene transcription, replication, and repair.

DOI: 10.46481/jnsps.2027.3527

Keywords: NMR relaxation times, Rare DNA intermediate structures, Wolfram Mathematica software, Statistical analysis, DNA secondary structures

Article History:
Received: 18 May 2026
Received in revised form: 05 July 2026
Accepted for publication: 10 September 2026
Available online: 26 October 2026

© 2027 The Author(s). Published by the Nigerian Society of Physical Sciences under the terms of the Creative Commons Attribution 4.0 International license. Further distribution of this work must maintain attribution to the author(s) and the published article's title, journal citation, and DOI.

Communicated by: C. A. Onate

1. Introduction

Rare DNA intermediate structures are essential for biological activities in living organisms. These DNA structures include, among others, G-quadruplexes, triplexes, and displacement loops (D-loops). In G-quadruplexes, each G-tetrad has four guanine bases linked by hydrogen bonds to form Hoogsteen base pairs [1–4]. A triplex is formed by extended purine or pyrimidine sequences on a DNA strand, with the third strand running parallel to the purine strand of the Watson–Crick base pairs [5, 6]. A D-loop results from homologous recombination, in which two strands of a double-stranded DNA molecule are separated and held apart by a third invading DNA strand [7].

Furthermore, the roles these structures play in living organisms include gene expression, transcription, and replication, which are controlled by G-quadruplexes [1–4, 8]. Triplexes are important in gene expression and recombination [5, 6], and D-loops are involved in DNA recombination and repair, transcription, and replication [9–11].

Similarly, nuclear magnetic resonance (NMR) is a non-invasive analytical technique with a short acquisition process that can be utilised to study the physical, chemical, and biological properties of DNA structures [12–18]. Applications include determination of protein structure, investigation of or-

*Corresponding Author Tel. No.: +234-806-634-5475.
Email address: johnalamkahlazarus@gmail.com (John A. Lazarus)

ganic molecules, and study of physical features at the molecular level, such as phase change, diffusion, solubility, and anatomical exchange, as well as structural dynamics and interactions of biomolecules [19–23]. However, statistical analysis of NMR parameters for DNA structures has been less studied. Therefore, this study presents a statistical analysis of NMR relaxation parameters (T_1 and T_2) for rare DNA intermediate structures.

2. Materials and methods

2.1. Materials

Materials utilised in this study include published experimental NMR relaxation data (T_1 and T_2) for rare DNA intermediates, simulated T_1 and T_2 NMR datasets for rare DNA intermediates, RStudio, and Wolfram Mathematica software.

2.1.1. Datasets

The datasets are shown in Table 1.

2.2. Methods

For robust and broad generalisation of the statistical-analysis results, datasets of 500 values for each rare DNA structure were utilised. The large datasets were simulated from experimental data obtained from previous studies (Table 1). This approach was used because generating large experimental datasets requires substantial resources, whereas simulated datasets are relatively inexpensive to obtain. Scripts in RStudio were used to generate the large datasets while maintaining a uniform system temperature for robust statistical analysis.

Therefore, G-quadruplex (telomeric) d[AGGG(TTAGGG)$_3$]–Tel22, hybrid topology, K^+ solution; G-quadruplex (c-MYC promoter) d(TGAGGGTGGGAGGGTGGGGAA)–Pu22T; G-quadruplex (bcl-2 promoter) d(GGGCGCGGGAGGAATTGGGCGGG); DNA triplex (parallel/antiparallel), dsDNA + triplex-forming oligonucleotide (TFO); and displacement loop, a 3-stranded invasion intermediate involving RecA/Rad51-mediated strand invasion, were used for the large datasets because they all have a uniform temperature of 25 °C. Wolfram Mathematica software was then used for statistical analysis of the 500-value datasets for each rare DNA intermediate structure. Abbreviated names for the five DNA structures are presented in Table 2.

The Anderson–Darling (A–D) goodness-of-fit (normality) test was applied to every group–parameter combination to select between parametric and non-parametric tests. The A–D test was preferred because it is relevant for relaxation-time datasets that exhibit long tails. The results of the A–D test required the use of non-parametric tests; the Kruskal–Wallis test was performed together with Dunn's post-hoc test. Also, Cohen's d, which quantifies effect size for each paired-group comparison, was calculated for all pairwise comparisons using the convention $|d| < 0.2$ = negligible, 0.2–0.5 = small, 0.5–0.8 = medium, and > 0.8 = large. This was done because statistical significance alone does not convey the practical magnitude of a difference, particularly when sample sizes are large.

3. Results

The probability-density plots and box-and-whisker plots for T_1 and T_2 relaxation times of the rare DNA intermediates are shown in Figure 1.

4. Discussion

Table 3 shows that every group rejects the null hypothesis of normality at a conventional significance threshold ($\alpha = 0.05$). The A–D statistics are very large (all > 40), reflecting large sample sizes.

As shown in Table 4, both T_1 and T_2 parameters yield p-values below 0.05, indicating statistically significant differences. Thus, at least one paired set of DNA structures differs in its T_1 or T_2 values and is not drawn from an identically distributed population.

From the results of Dunn's test in Table 5, for T_1, Tel22 vs Triplex and Tel22 vs D-Loop are significant. This implies that the T_1 values for the two paired groups are respectively different and could be used to isolate each paired structure. For T_2, all comparisons except Tel22 vs Pu22T, Tel22 vs bcl-2, and Pu22T vs bcl-2 are significant. This indicates that the T_2 values for each structure in these three paired groups do not show a statistically significant difference. This could be because all the paired structures belong to the same structural class of G-quadruplex.

In Table 6, for T_1, Tel22 vs Pu22T, Tel22 vs bcl-2, Tel22 vs Triplex, and Tel22 vs D-Loop have the highest Cohen's d values, with Tel22 vs Triplex being the largest ($|d| = 1.215$). These are followed by Pu22T vs Triplex and Triplex vs D-Loop; the remaining comparisons have smaller values, with Pu22T vs D-Loop having the smallest Cohen's d value ($|d| = 0.049$).

For T_2, Pu22T vs D-Loop, bcl-2 vs D-Loop, Triplex vs D-Loop, Tel22 vs Triplex, Tel22 vs D-Loop, Pu22T vs Triplex, and bcl-2 vs Triplex have large values; with Triplex vs D-Loop being the highest ($|d| = 2.878$). Tel22 vs Pu22T and Tel22 vs bcl-2 have medium values; and Pu22T vs bcl-2 has a negligible Cohen's d value, which is the lowest ($|d| = 0.036$), implying a smaller effect between the paired groups. In addition, the lowest Cohen's d value for T_1 ($|d| = 0.049$) is higher than that for T_2 ($|d| = 0.036$).

In Figure 1(a), the density distributions of T_1 overlap, which implies that spin–lattice interactions occur among the DNA structures and indicates the possibility of energy exchange among the structures. For T_2, the peaks are differentiated and narrow, with the purple curve being the narrowest. This indicates rapid spin–spin dephasing as a result of restricted movement of the structures, especially in D-Loop. Overall, the different colours indicate distinct molecular conformations of the DNA structures, and a transition from one structure may overlap with another and could alter the flexibility of that structure.

As shown in Figure 1(b), the box-and-whisker plots show T_1 (left) and T_2 (right) relaxation times for each DNA secondary structure. Boxes span the interquartile range (Q1–Q3); internal lines indicate the median; diamond markers indicate

Table 1: Published experimental T_1 and T_2 datasets for rare DNA intermediate structures.

Rare DNA intermediate	Sequence	Nucleus	Field (MHz)	Temp. (°C)	T_1 (s)	T_2 (ms)
G-quadruplex (telomeric) d[AGGG(TTAGGG)$_3$]–Tel22, hybrid topology, K^+ solution [24]	26-nt intramolecular; ~8 kDa	^{1}H (imino)	600	25	0.3–1.2	10–45
G-quadruplex (c-MYC promoter) d(TGAGGGTGGGAGGGTGGGGAA)–Pu22T [24]	22-nt intramolecular G4; ~7 kDa	^{1}H (imino)	600	25	0.5–1.5	15–50
G-quadruplex (bcl-2 promoter) d(GGGCGCGGGAGGAATTGGGCGGG) [24]	23-nt intramolecular G4	^{1}H (imino)	600	25	0.5–1.5	15–50
i-Motif (C-rich, pH 7), intercalated cytosine-tetrad quadruplex [25]	~20–24 nt; pH 7 near-neutral form	^{1}H	600	5	0.8–2.0	20–80
DNA triplex (parallel/antiparallel), dsDNA + triplex-forming oligonucleotide (TFO) [26]	14-mer duplex + 10-mer TFO; pH 5.5	^{1}H	800	25	0.6–1.5	20–70
Displacement loop: 3-stranded invasion intermediate; RecA/Rad51-mediated strand invasion [27]	~50–80 bp total; ~40 kDa	^{1}H	500–600	25	0.5–1.5	2–15

Table 2: Abbreviated names for the rare DNA intermediates (secondary structures) utilised for analysis.

S/N	Full name/sequence	Structural class	Abbreviation
1	G-quadruplex (telomeric): d[AGGG(TTAGGG)$_3$], hybrid topology, K^+ solution	G-quadruplex	Tel22
2	G-quadruplex (c-MYC promoter): d(TGAGGGTGGGAGGGTGGGGAA)	G-quadruplex	Pu22T
3	G-quadruplex (bcl-2 promoter): d(GGGCGCGGGAGGAATTGGGCGGG)	G-quadruplex	bcl-2
4	DNA triplex: dsDNA + parallel/antiparallel triplex-forming oligonucleotide (TFO)	Triple helix	Triplex
5	Displacement loop: 3-stranded invasion intermediate; RecA/Rad51-mediated strand invasion	Displacement loop	D-Loop

Table 3: Anderson–Darling (A–D) normality-test results for all groups and parameters.

Group	Parameter	A–D statistic	p-value	Normal
Tel22	T_1 (s)	55.91	1.33×10^{-15}	No
Tel22	T_2 (s)	40.64	≈ 0	No
Pu22T	T_1 (s)	76.80	7.77×10^{-16}	No
Pu22T	T_2 (s)	40.60	≈ 0	No
bcl-2	T_1 (s)	81.60	1.44×10^{-15}	No
bcl-2	T_2 (s)	40.59	4.44×10^{-16}	No
Triplex	T_1 (s)	85.18	3.22×10^{-15}	No
Triplex	T_2 (s)	40.23	≈ 0	No
D-Loop	T_1 (s)	78.72	6.66×10^{-16}	No
D-Loop	T_2 (s)	41.00	1.11×10^{-15}	No

Table 4: Kruskal–Wallis test results for T_1 and T_2 relaxation times for rare DNA intermediate structures.

Parameter	H-statistic	Degrees of freedom	p-value	Significant ($\alpha = 0.05$)	Interpretation
T_1	16.93	4	2.0×10^{-3}	Significant	At least one group differs in T_1
T_2	65.83	4	1.72×10^{-15}	Significant	At least one group differs in T_2

the group mean; and whiskers extend to the most extreme values within $1.5 \times$ IQR of the quartiles. No outliers are present in

Table 5: Dunn's test results for T_1 and T_2 relaxation times for rare DNA intermediate structures.

	T_1					T_2				
Comparison	Rank diff.	z	p	Adj. p	Sig.	Rank diff.	z	p	Adj. p	Sig.
Tel22 vs Pu22T	17.79	1.61	0.1067	1.0000	No	9.21	0.835	0.4039	1.0000	No
Tel22 vs bcl-2	28.59	2.59	0.0096	0.0955	No	10.93	0.991	0.3217	1.0000	No
Tel22 vs Triplex	34.45	3.12	0.0018	0.0179	Yes	47.52	4.308	1.65×10^{-5}	1.65×10^{-4}	Yes
Tel22 vs D-Loop	40.90	3.71	0.0002	0.0021	Yes	42.66	3.867	1.10×10^{-4}	1.10×10^{-3}	Yes
Pu22T vs bcl-2	10.79	0.98	0.3278	1.0000	No	1.72	0.156	0.8758	1.0000	No
Pu22T vs Triplex	16.66	1.51	0.1311	1.0000	No	38.31	3.473	5.14×10^{-4}	5.14×10^{-3}	Yes
Pu22T vs D-Loop	23.10	2.09	0.0362	0.3621	No	51.87	4.702	2.58×10^{-6}	2.58×10^{-5}	Yes
bcl-2 vs Triplex	5.86	0.53	0.5951	1.0000	No	36.59	3.317	9.10×10^{-4}	9.10×10^{-3}	Yes
bcl-2 vs D-Loop	12.31	1.12	0.2644	1.0000	No	53.59	4.858	1.19×10^{-6}	1.19×10^{-5}	Yes
Triplex vs D-Loop	6.45	0.58	0.5588	1.0000	No	90.18	8.175	$< 1.00 \times 10^{-15}$	$< 1.00 \times 10^{-14}$	Yes

Table 6: Cohen's d effect sizes for T_1 and T_2 relaxation times for rare DNA intermediates.

	T_1				T_2			
Comparison	Upper	Lower	Cohen's d	Magnitude	Upper	Lower	Cohen's d	Magnitude
Tel22 vs Pu22T	1.031	0.771	0.901	Large	0.650	0.398	0.524	Medium
Tel22 vs bcl-2	1.218	0.952	1.085	Large	0.611	0.359	0.485	Medium
Tel22 vs Triplex	1.350	1.080	1.215	Large	1.682	1.400	1.541	Large
Tel22 vs D-Loop	1.099	0.837	0.968	Large	1.734	1.450	1.592	Large
Pu22T vs bcl-2	0.283	0.035	0.159	Negligible	0.160	0.088	0.036	Negligible
Pu22T vs Triplex	0.385	0.137	0.261	Small	1.225	0.959	1.092	Large
Pu22T vs D-Loop	0.173	0.075	0.049	Negligible	2.297	1.987	2.142	Large
bcl-2 vs Triplex	0.225	0.023	0.101	Negligible	1.252	0.986	1.119	Large
bcl-2 vs D-Loop	0.235	0.013	0.111	Negligible	2.245	1.937	2.091	Large
Triplex vs D-Loop	0.338	0.090	0.214	Small	3.055	2.701	2.878	Large

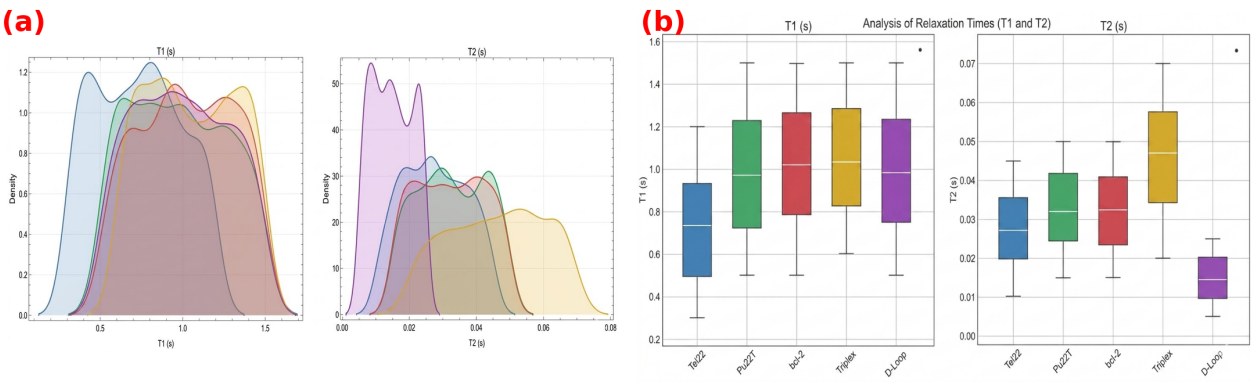

Figure 1: Distribution of relaxation times for rare DNA intermediates showing (a) kernel density estimate (KDE) overlays and (b) box-and-whisker plots.

any group.

Figure 2 shows the correlation between T_1 and T_2 for the five DNA structures. The correlation indicates the independence of the T_1 and T_2 transitions that occur in each structure without interference.

Figure 3 shows that colour intensity encodes local probability density. Elongation along the T_1 axis reflects the larger absolute variance in longitudinal relaxation; the joint distribution shape reveals any T_1–T_2 covariance specific to each structural class. The blue colour indicates a region with a low concentration of protons and hence a region of minimum interaction; yellow indicates an intermediate concentration of protons, where there is slight interaction due to proton availability; and red indicates a high concentration of protons and a region of maximum interaction in the DNA structures.

In Figure 4, fifteen contour levels are drawn at equally spaced density thresholds. Contour eccentricity and orientation encode the direction and strength of T_1–T_2 correlation within each group. Logarithmic axes compress long-tail features and render multiplicative structure visible as additive displacement.

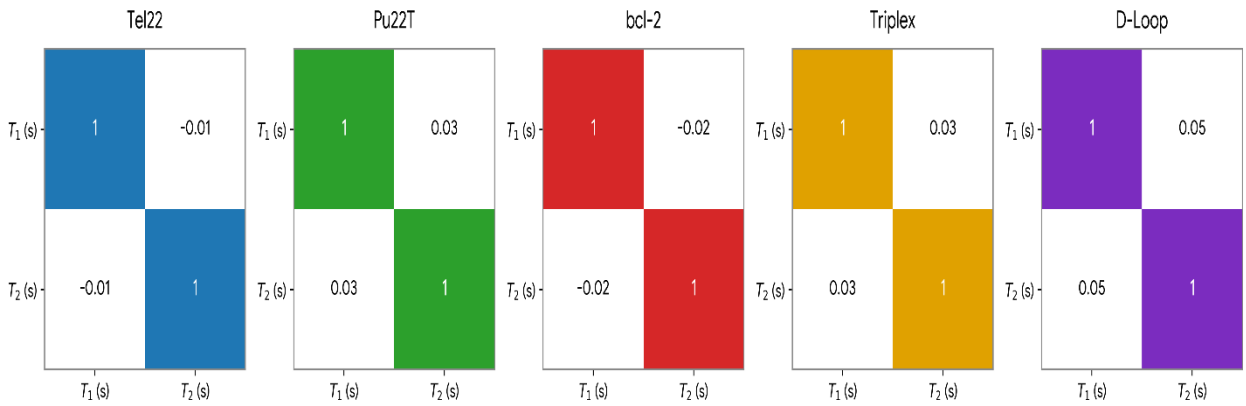

Figure 2: Pearson correlation matrices of the T_1 and T_2 relaxation times for rare DNA intermediates.

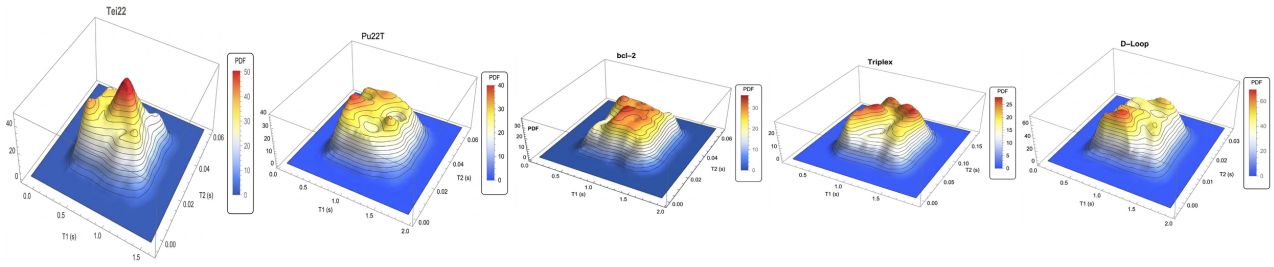

Figure 3: Three-dimensional smooth density heatmaps in T_1–T_2 space for rare DNA intermediate structures.

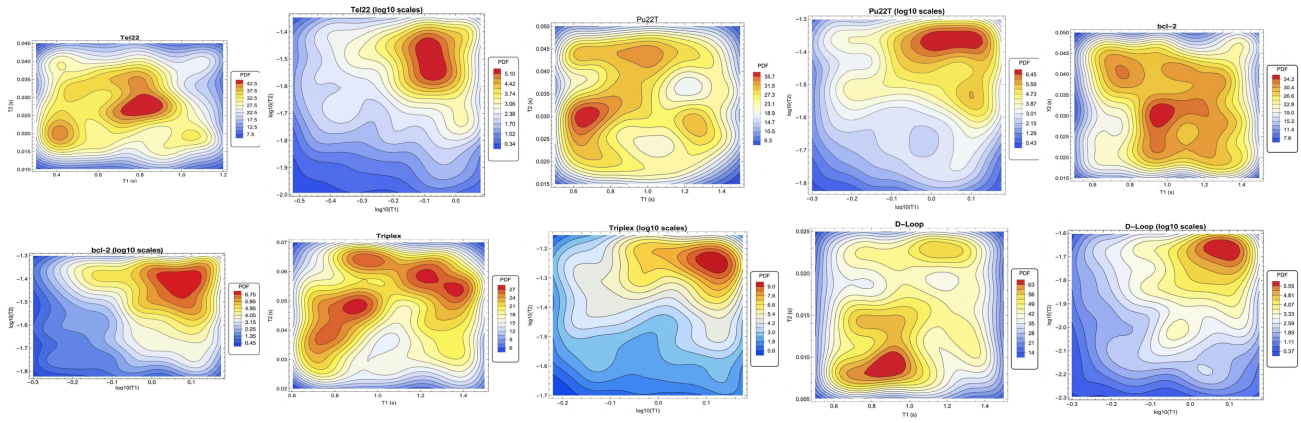

Figure 4: Contour plots of bivariate smooth kernel density estimates in T_1–T_2 space for rare DNA intermediates on linear and $\log_{10}$ scales.

The red, yellow, and blue colours are regions of high, moderate, and low nucleic acid base density and indicate tight, transient, and loose bond regions within the DNA structures, respectively. This makes classification of rare intermediate structures possible.

5. Conclusion

The study presents a statistical analysis of simulated datasets of NMR longitudinal (T_1) and transverse (T_2) relaxation times for five rare DNA intermediate structures using Wolfram Mathematica software. Due to the non-normal distributions of the datasets, non-parametric statistical methods were adopted for the analysis. Results show that T_1 and T_2 values for each of the five rare DNA structures possess distinct features. This highlights the possibility of utilising DNA T_1 and T_2 NMR data to isolate DNA structures.

Nucleic acid base density determines base sequence, and DNA structure is influenced by base sequence [28]. Also, DNA structures are responsible for regulating gene transcription, replication, and repair [28, 29]. Although the study utilised simulated datasets, these could result in overfitting or underfitting of the statistical results. Therefore, validation with

experimental results from large datasets is needed before adoption for genomic applications.

Data availability

The R script used to simulate large datasets from experimental data and the simulated datasets for rare DNA intermediate structures utilised in the present study are available from the corresponding author upon reasonable request.

Declaration of competing interest

The authors declare that they have no known competing financial interests or personal relationships that could have appeared to influence the work reported in this manuscript.

Funding

The authors received no specific funding from any public, commercial, or not-for-profit organisation for this research.

Acknowledgment

The authors sincerely appreciate the management of Federal University of Technology, Minna, Niger State, Nigeria, for the opportunity to carry out the study.

References

[1] J. Sun, Y. Wang, Y. Huang & Z. Chen, "G-quadruplex unwinding molecular mechanisms by helicases and their applications", International Journal of Molecular Sciences **27** (2026) 1629. https://doi.org/10.3390/ijms27041629.

[2] E. Soorya & S. S. Pingale, "DFT analysis of stacking interactions and cyclic H-bond cooperativity in G-quadruplexes", Journal of Computational Chemistry **46** (2025) e70290. https://doi.org/10.1002/jcc.70290.

[3] A. L. Soenarjo, Z. Lan, I. V. Sazanovich, Y. S. Chan, M. Ringholm, A. Jha & D. R. Klug, "The transition from unfolded to folded G-quadruplex DNA analyzed and interpreted by two-dimensional infrared spectroscopy", Journal of the American Chemical Society **145** (2023) 19622. https://doi.org/10.1021/jacs.3c04044.

[4] J. Y. Gong, C. J. Wen, M. L. Tang, R. F. Duan, J. N. Chen, J. Y. Zhang, K. W. Zheng, Y. D. He, Y. H. Hao, Q. Yu, S. P. Ren & Z. Tan, "G-quadruplex structural variations in human genome associated with single-nucleotide variations and their impact on gene activity", Proceedings of the National Academy of Sciences of the United States of America **118** (2021) e2013230118. https://doi.org/10.1073/pnas.2013230118.

[5] S. Rhee, Z. J. Han, K. Liu, H. T. Miles & D. R. Davies, "Structure of a triple helical DNA with a triplex-duplex junction", Biochemistry **38** (1999) 16810. https://doi.org/10.1021/bi991811m.

[6] M. D. Frank-Kamenetskii & S. M. Mirkin, "Triplex DNA structures", Annual Review of Biochemistry **64** (1995) 65. https://doi.org/10.1146/annurev.bi.64.070195.000433.

[7] I. Kovalchuk & O. Kovalchuk (Eds.), *Genome Stability: From Virus to Human Application*, 2nd edition, Academic Press, Amsterdam, Netherlands, 2021, pp. 117–131. https://doi.org/10.1016/C2020-0-00641-9.

[8] J. Robinson, F. Raguseo, S. P. Nuccio, D. Liano & M. Di Antonio, "DNA G-quadruplex structures: more than simple roadblocks to transcription?", Nucleic Acids Research **49** (2021) 8419. https://doi.org/10.1093/nar/gkab609.

[9] L. Joudeh, R. E. Appleby, J. D. Maman & L. Pellegrini, "Structural mechanism of strand exchange by the RAD51 filament", eLife **14** (2025) RP107114. https://doi.org/10.7554/eLife.107114.

[10] B. H. Annex & R. S. Williams, "Mitochondrial DNA structure and expression in specialized subtypes of mammalian striated muscle", Molecular and Cellular Biology **10** (1990) 5671. https://doi.org/10.1128/mcb.10.11.5671-5678.1990.

[11] J. N. Doda, C. T. Wright & D. A. Clayton, "Elongation of displacement-loop strands in human and mouse mitochondrial DNA is arrested near specific template sequences", Proceedings of the National Academy of Sciences of the United States of America **78** (1981) 6116. https://doi.org/10.1073/pnas.78.10.6116.

[12] J. M. Yang, J. Kim, Y. Lee, W. Lee & J. C. Park, "NMR structure and biophysical characterization of thermophilic single-stranded DNA binding protein from *Sulfolobus solfataricus*", International Journal of Molecular Sciences **23** (2022) 3099. https://doi.org/10.3390/ijms23063099.

[13] C. A. Brosey, S. E. Soss, S. Brooks, C. Yan, I. Ivanov, K. Dorai & W. J. Chazin, "Functional dynamics in replication protein A DNA binding and protein recruitment domains", Structure **23** (2015) 1028. https://doi.org/10.1016/j.str.2015.04.008.

[14] C. Brown, K. Campos-Leon, M. Strickland, C. Williams, V. S. S. Fairweather, R. L. Brady, M. P. Crump & K. Gaston, "Protein flexibility directs DNA recognition by the papillomavirus E2 proteins", Nucleic Acids Research **39** (2011) 2969. https://doi.org/10.1093/nar/gkq1217.

[15] L. E. Thompson & D. Rovnyak, "Accessible NMR experiments studying the hydrodynamics of ^{15}N-enriched ubiquitin at low fields", Biochemistry and Molecular Biology Education **35** (2007) 49. https://doi.org/10.1002/bmb.23.

[16] C. Castagné, E. C. Murphy, A. M. Gronenborn & M. Delepierre, "^{31}P NMR analysis of the DNA conformation induced by protein binding: SRY/DNA complexes", European Journal of Biochemistry **267** (2000) 1223. https://doi.org/10.1046/j.1432-1327.2000.01124.x.

[17] R. Sahu, A. Kumar, R. Mishra, C. Majee & R. Kumar, "Recent development in nuclear magnetic resonance as a technique for quantitative method validation", Indian Journal of Pharmaceutical Sciences **83** (2021) 1094. https://doi.org/10.36468/pharmaceutical-sciences.865.

[18] O. B. Awojoyogbe, M. O. Dada, O. P. Faromika & O. E. Dada, "Mathematical concept of the Bloch flow equations for general magnetic resonance imaging: A review", Concepts in Magnetic Resonance Part A **38A** (2011) 85. https://doi.org/10.1002/cmr.a.20210.

[19] E. Bairaktari, K. Katopodis, K. C. Siamopoulos & O. Tsolas, "Paraquat-induced renal injury studied by ^{1}H nuclear magnetic resonance spectroscopy of urine", Clinical Chemistry **44** (1998) 1256. https://doi.org/10.1093/clinchem/44.6.1256.

[20] R. W. Darbeau, "Nuclear magnetic resonance (NMR) spectroscopy: A review and a look at its use as a probative tool in deamination chemistry", Applied Spectroscopy Reviews **41** (2006) 401. https://doi.org/10.1080/05704920600726175.

[21] G. Patel & D. Chudasama, "Nuclear magnetic resonance spectroscopy NMR", Journal of Nuclear Engineering & Technology **11** (2021) 30. https://www.researchgate.net/publication/357735866_Nuclear_Magnetic_Resonance_Spectroscopy_NMR.

[22] D. Marion, "An introduction to biological NMR spectroscopy", Molecular & Cellular Proteomics **12** (2013) 3006. https://doi.org/10.1074/mcp.O113.030239.

[23] P. J. Sapienza & A. L. Lee, "Using NMR to study fast dynamics in proteins: methods and applications", Current Opinion in Pharmacology **10** (2010) 723. https://doi.org/10.1016/j.coph.2010.09.006.

[24] A. Ambrus & D. Yang, "Diffusion-ordered nuclear magnetic resonance spectroscopy for analysis of DNA secondary structural elements", Analytical Biochemistry **367** (2007) 56. https://doi.org/10.1016/j.ab.2007.04.025.

[25] H. Abou Assi, M. Garavís, C. González & M. J. Damha, "i-Motif DNA: structural features and significance to cell biology", Nucleic Acids Research **46** (2018) 8038. https://doi.org/10.1093/nar/gky735.

[26] Y. Huang, *Development of antisense alpha-helical peptide nucleic acids, Ph.D. dissertation*, Department of Chemistry, Case Western Reserve University, Cleveland, Ohio, 2002. https://www.proquest.com/openview/837b212f801191c2059c70bc780e04e8/1?pq-origsite=gscholar&cbl=18750&diss=y

[27] D. M. J. Lilley & D. G. Norman, "The Holliday junction is finally seen with crystal clarity", Nature Structural Biology **6** (1999) 897. https://doi.org/10.1038/13255.

[28] A. Bansal, S. Kaushik & S. Kukreti, "Non-canonical DNA structures: diversity and disease association", Frontiers in Genetics **13** (2022) 959258. https://doi.org/10.3389/fgene.2022.959258.

[29] F. Y. Teng, Z. Z. Jiang, M. Guo, X. Z. Tan, F. Chen, X. G. Xi & Y. Xu, "G-quadruplex DNA: a novel target for drug design", Cellular and Molecular Life Sciences **78** (2021) 6557. https://doi.org/10.1007/s00018-021-03921-8.